Comprehensive analysis on the effects of noise estimation strategies on image noise artifact suppression performance

Angus Leigh, Alexander Wong, David A. Clausi, and Paul Fieguth
Department of Systems Design Engineering
University of Waterloo, Canada
{*adleigh, a28wong, dclausi, pfieguth*}@*uwaterloo.ca*

***Abstract*—In this paper, the effects of employing different noise estimation strategies on the performance of noise artifact suppression techniques in achieving high image quality has been investigated. Most literature on the subject tends to use the true noise level of the noisy image when performing noise artifact suppression. However, this approach does not reflect how such techniques would be used in practical situations where the true noise level is unknown, which is common in most image and video processing applications. Therefore, in practical situations, the noise level must first be estimated before a noise artifact suppression technique can be applied using the estimated noise level. Through a comprehensive analysis of different noise estimation strategies using empirical testing on a variety of images with different characteristics, the MAD wavelet noise estimation technique was found to be the overall preferred noise estimation technique for all popular noise artifact suppression techniques investigated (BM3D, bilateral, NeighShrink, BLS-GSM and non-local means). Furthermore, the BM3D noise artifact suppression technique, combined with the MAD wavelet noise estimation technique, was found to offer the best performance in achieving high image quality in situations where the noise level is unknown and must be estimated. The outcome of this research is clear recommendations that can be used in practise when suppressing noise artifacts exhibited in digital imagery and video.**

***Keywords*-image noise artifact suppression; noise estimation; image and video processing**

I. Introduction

A continuous area of research in the field of image and video processing is noise artifact suppression, where an image or video that has been contaminated by some form of noise is processed in an attempt to recover the original image or video. Noise artifact suppression has numerous image and video processing applications including photographic enhancement, video enhancement, edge detection [1], object recognition [2] and video tracking [3]. Given the importance of noise artifact suppression on various image and video processing applications, many different noise artifact suppression techniques have been presented over the years and while significant progress has and is continually being made, no techniques have completely addressed this problem.

In literature pertaining to image noise artifact suppression it is often assumed that noise present in images is additive white Gaussian noise. In this way, the intensity of noise can be specified in terms of its standard deviation σ. This value is the most important parameter in virtually all image noise artifact suppression techniques as it has the greatest effect on the overall quality of the denoised image. The overestimation of the noise level typically leads to excessive smoothing of the image and loss of image detail, while the underestimation of the noise level results in insufficient noise removal.

When images are denoised in practical, real-world situations the exact value of the noise standard deviation is unknown and must be estimated. However, in much of existing research literature, noise artifact suppression techniques are commonly tested using the true noise level of the image. One significant effect this method of testing fails to take into consideration is the robustness of the noise artifact suppression techniques to the noise level determined using a noise estimation strategy, which is often inaccurate when compared to the true noise level. For example, some noise artifact suppression techniques may appear to perform better than others when the exact true noise level is used as the input parameter, but other techniques might perform better in practice when the noise level must be estimated since they are more robust to inaccurate input noise levels.

The purpose of this paper is to perform a comprehensive analysis that explores the effects of using different noise estimation strategies on the performance of noise artifact suppression techniques and on final denoised image quality. The rest of the paper is organized as follows. A background overview on noise estimation strategies as well as popular noise artifact suppression methods are presented in Section II. The methodology used in the comprehensive analysis is described in Section III. Experimental results are presented and discussed in Section IV. Finally, conclusions are drawn in Section V.

II. Background

While image noise artifact suppression techniques have been thoroughly studied in the research literature, noise estimation techniques are not as prevalent. The existing estimation techniques can either be classified as those which look at multiple images from the same source to estimate the intensity of noise and those which use only one image to estimate the intensity of noise. In this study, we will focus on noise estimation techniques that use only a single image.

For this study, let us assume that an observed, noisy image g of size $N \times M$ is composed of the noise-free image f and an additive white Gaussian noise source n following the distribution $\mathcal{N}(0, \sigma^2)$, where σ^2 is the noise variance,

$$g(x, y) = f(x, y) + n(x, y). \tag{1}$$

One class of noise estimation techniques make use of wavelet characteristics to estimate the noise variance in the image. A common wavelet-based technique for estimating the parameter σ is the median absolute deviation (MAD) method, which is based on the assumption that the MAD of the wavelet coefficients of g in the highest frequency subband is proportional to the noise standard deviation [4], [5], which can be defined as

$$\hat{\sigma}_{noise,MAD} = \frac{1}{0.6745} \times MAD(y^H_{i,j}) \tag{2}$$

where $y^H_{i,j}$ are the wavelet coefficients in the highest frequency subband. The MAD operation, for some dataset X_i, is defined as the median of the absolute deviations from the median of the dataset:

$$MAD = Median_i(\|X_i - Median_j(X_j)\|). \tag{3}$$

Another class of noise estimation techniques use local variances of pixel intensity to estimate the noise variance in the image. This involves starting at a position on the image and calculating the variance of pixel intensity of all pixels within a specified range. The position is then shifted by one pixel and the process is repeated until the local variances are known for all possible positions on the image. Using this approach, one common technique is to use the mean of the local variances as the noise variance of the image,

$$\hat{\sigma}_{noise,meanlv} = \frac{1}{NM} \sum_x \sum_y \left[(g^2(x, y) * w) - (g(x, y) * w)^2 \right] \tag{4}$$

where $*$ denotes a convolution and w is a box kernel of size $S \times S$. Other common noise estimation techniques based on local variances include using the maximum, minimum, median, and mode local variances as the noise variance of the image,

$$\hat{\sigma}_{noise,minlv} = Min \left[(g^2(x, y) * w) - (g(x, y) * w)^2 \right], \tag{5}$$

$$\hat{\sigma}_{noise,maxlv} = Max \left[(g^2(x, y) * w) - (g(x, y) * w)^2 \right], \tag{6}$$

$$\hat{\sigma}_{noise,medlv} = Median \left[(g^2(x, y) * w) - (g(x, y) * w)^2 \right], \tag{7}$$

$$\hat{\sigma}_{noise,modelv} = Mode \left[(g^2(x, y) * w) - (g(x, y) * w)^2 \right]. \tag{8}$$

In terms of image noise artifact suppression techniques, they can either be classified as spatial techniques or transform techniques. Spatial techniques analyze and modify the pixel intensity values directly while transform techniques transform the image into another domain, such as the Fourier domain, and then analyze and modify the resulting spectrum before transforming the image back to the spatial domain.

One of the current leading spatial techniques is the bilateral filter [6]. It is an extension of the Gaussian smoothing filter, which replaces the value of each pixel with a weighted average of nearby pixel values with the weighting being dependent on spatial proximity. The bilateral filter extends on this by basing the weights not only on spatial proximity, but also on similarities in pixel intensities, where pixels with more similar pixel intensities begin assigned a higher weight. This results in the bilateral filter having significantly better edge preservation than the Gaussian smoothing filter. To further improve noise artifact suppression performance in the spatial domain, the non-local means filter [7] was introduced, and is considered one of the leading edge spatial techniques available. A non-local technique, the non-local means filter utilizes redundant structures throughout the noisy image to estimate the original image.

Some of the leading transform techniques include the Bayes least squares-Gaussian scale mixture (BLS-GSM) filter [8], BM3D filter [9] and the NeighShrink filter [10]. More specifically, the BLS-GSM and NeighShrink filters are wavelet techniques, where coefficients in the decomposed wavelet sub-bands that are associated with noise energy are suppressed. The BM3D technique is a non-local technique that utilizes groups of similar structures and employs them to perform noise artifact suppression in a collaborative transform domain.

In this comprehensive analysis, all of the aforementioned noise estimation strategies and noise artifact suppression techniques are considered to examine the effects of using different noise estimation strategies on both types of noise artifact suppression techniques for different types of images.

When using these techniques in practice one would first take a noisy image and use a noise estimation technique to estimate the intensity of noise present and then use a noise artifact suppression technique with the noise level used as a parameter to denoise the image. Where maximum denoised image quality is the goal, pertinent questions that would then arise would be:

1) Which noise estimation technique results in the best performance for each noise artifact suppression technique?
2) Which noise artifact suppression technique performs best when an estimated noise level is used?

(a) AERIAL (256x256)

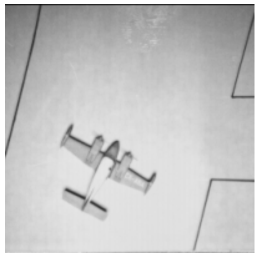

(b) AIRPLANE (256x256)

(c) BARBARA (512x512)

(d) BOAT (512x512)

(e) CAMERAMAN (256x256)

(f) CLOCK (256x256)

(g) COUPLE (512x512)

(h) FACTORY (256x256)

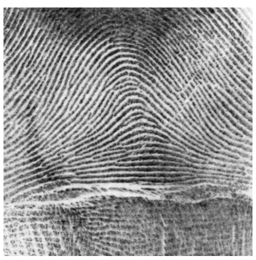

(i) FINGERPRINT (512x512)

(j) HILLS (512x512)

(k) HOUSE (256x256)

(l) LENA (512x512)

(m) LENA (256x256)

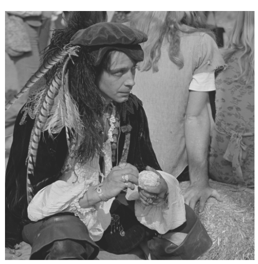

(n) MAN (512x512)

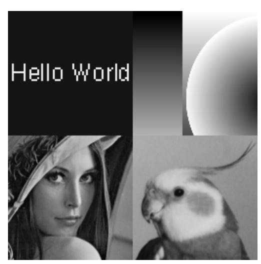

(o) MONTAGE (256x256)

(p) MOON (256x256)

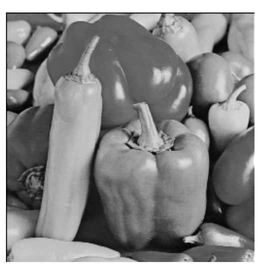

(q) PEPPERS (256x256)

Figure 1. Test images used in the comprehensive analysis.

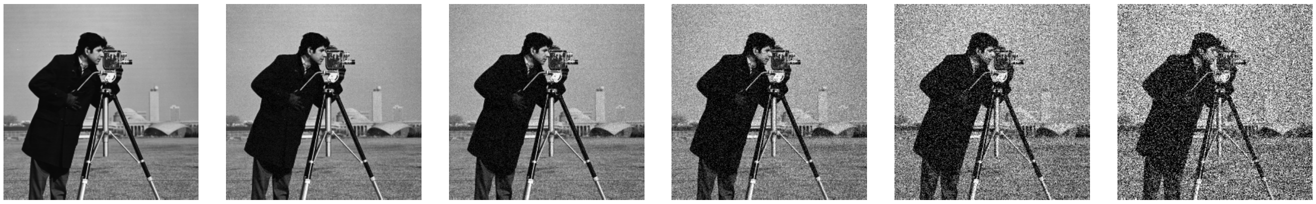

(a) Original image with no noise (b) $\sigma_{applied}$ = 5, PSNR = 34.1dB (c) $\sigma_{applied}$ = 10, PSNR = 28.3dB (d) $\sigma_{applied}$ = 20, PSNR = 22.4dB (e) $\sigma_{applied}$ = 40, PSNR = 16.6dB (f) $\sigma_{applied}$ = 60, PSNR = 13.5dB

Figure 2. Sample noise application to CAMERMAN image.

III. METHODOLOGY

One possible approach to measuring the performance of noise estimation techniques is to apply them to a noisy image where the true noise level (σ_{true}) is known and compare the resulting estimated noise ($\hat{\sigma}_{noise}$) with σ_{true}. We opted to not to use this approach for this study because when estimators are coupled with noise artifact suppression techniques their individual contributions are masked. For example, there may be an estimation technique that consistently overestimates the noise level that is combined with a noise artifact suppression technique that performs well with overestimated noise levels but together they still produce high quality denoised images. For this reason, we used the difference in the final image quality as the performance metric for the estimators, rather than directly comparing $\hat{\sigma}_{noise}$ with σ_{true}.

To determine which noise estimation technique offers the best performance for each denoising technique we first gathered a sample of 17 stock greyscale images, ten of which were 256×256 pixels in size (AERIAL, AIRPLANE, CAMERMAN, CLOCK, FACTORY, HOUSE, LENA, MONTAGE, MOON and PEPPERS) and seven of which were 512×512 pixels in size (BARBARA, BOAT, COUPLE, FINGERPRINT, HILL, LENA and MAN). This set of test images, shown in Fig. 1, was chosen with a sizable variety so that it would be possible to reasonably generalize the results. Noisy images were then created by contaminating the stock images with different degrees of additive white Gaussian noise. We used standard deviations of $\sigma_{applied}$ = 5, 10, 20, 40 and 60 for the contaminating noise so a wide range of different noise levels would be covered. Note that the pixel intensities had to be constrained to values between 0 and 255 after the noise was applied, thus the resulting σ_{true} in the images was usually slightly less than $\sigma_{applied}$. A sample of the resulting noisy images is shown in Figure 2.

With each of the stock noisy images, we first determined the optimal noise parameter σ_{opt} for each noise suppression technique that maximizes the peak signal-to-noise ratio (PSNR) achieved for that technique,

$$\sigma_{opt} = \arg\max_{\sigma} PSNR(\sigma). \tag{9}$$

The value σ_{opt} was obtained via a search technique where we inputted incremental values from 0 up to 80 for the σ parameter into each of the noise artifact suppression techniques, covering the range we would expect the maximum PSNR to occur in. As an aside, we noticed that σ_{opt} usually occurred within 1 value of σ_{true} and returned a PSNR that was usually no greater than 1% of the value returned from when using σ_{true}.

The denoised images were then evaluated to determine the PSNR achieved using the estimated noise parameter $\hat{\sigma}_{noise}$. To evaluate the performance of each noise estimation method in a quantitative manner, we computed the ratio between the PSNR achieved using the estimated noise parameter $\hat{\sigma}_{noise}$ and the PSNR achieved using the optimal noise parameter σ_{opt},

$$perf = \frac{PSNR(\hat{\sigma}_{noise})}{PSNR(\sigma_{opt})}. \tag{10}$$

There are two main advantages to using such a performance metric. First, such a performance metric allows for easy interpretation of the relative performance of the noise estimation methods. Second, this performance metric makes it possible to average the results across all images. Plots of this performance metric for the different noise estimation methods when used with different noise artifact suppression techniques are shown in Figures 3 and 4.

To determine the best noise artifact suppression technique when using an estimated noise level we utilized the results from the previous test that showed which is the preferred estimation technique for each noise artifact suppression technique. We then simply ran each noise artifact suppression technique on each of the noisy stock images using an estimated noise level generated from the preferred noise estimation technique. The denoised images were then evaluated for their PSNR and the results were averaged across all stock images.

Each of the noise artifact suppression algorithms was implemented in MATLAB and was acquired through existing libraries available online. We kept as much of the default configurations as possible for each noise artifact suppression algorithm with the exception of the bilateral filter. It required significant configuration because rather than having a straightforward input parameter for the noise level, as with the other techniques, it requires a spatial parameter σ_s, which may remain fixed, and an intensity parameter σ_i, which should be based on the noise level. There are no universally agreed optimal values for these but we found best results when using a spatial parameter of $\sigma_s = 3$ and an intensity parameter of $\sigma_i = 1.95 \times \sigma_{noise}$. These are also the values recommended in [11]. Finally, each of the noise estimation methods were implemented in MATLAB as well, with the Daubechies 4 (db4) wavelet transform used for the MAD noise estimation method [4], [5], and a 7×7 normalized box kernel used for w for the noise estimation methods based on local variances.

IV. Results

Subfigures (a) to (e) of Fig. 3 show the performances of the estimation techniques for each noise artifact suppression technique and for each level of applied noise. The results in these subfigures would be useful to someone who has selected a noise artifact suppression technique and knows the general amount of noise in an image so they could select an estimation technique that performs the best for that general noise range. In these subfigures we can see that the MAD wavelet and the mode variance techniques performed the best overall and consistently produced images with quality that was within 5% of the maximum PSNR across all levels of noise. We can also see that the minimum and maximum variance techniques resulted in overall very poor performance while the mean and median variance techniques performed reasonably well in general.

The data from the subfigures in Fig. 3 is further summarized in Fig. 4 where the performances of the estimation techniques are averaged across all five levels of applied noise. This gives a more general idea of how well each noise estimation technique performs when used with each noise artifact suppression technique across a wide range of noise levels.

From this figure we can see a fairly consistent pattern across all noise artifact suppression techniques were the MAD wavelet technique offers the best overall performance, followed by the mode variance, median variance, mean variance and finally, with maximum and minimum variance returning the overall poorest results.

The computational requirements for all estimation techniques was quite low as each estimation was completed in well under one second per image.

Fig. 5 provides an illustrative answer to the question regarding which noise artifact suppression technique performs the best when using an estimated noise level. From the results in Question 1 we knew that the MAD noise estimator resulted in the overall best performance for all noise artifact suppression techniques, thus it was the noise estimator used for their comparison. The test showed that the BM3D noise artifact suppression technique combined with the MAD noise estimator performed the best overall since it produced the highest PSNR images in all noise levels. In contrast, the bilateral filter had the lowest average performance of the tested methods. In this figure it can also be observed that the relative performance of each noise artifact suppression technique is consistent across the noise levels.

The computational requirements of BM3D, bilateral, BLS-GSM and Neighshrink were all fairly mild as each was able to denoise a 512×512 pixel image in under 20 seconds. Non-local means, however, was drastically more demanding and usually required an order of magnitude more computational time.

V. Conclusion

In this paper we carried out a comprehensive analysis to explore the effects of different noise estimation strategies on the performance of noise artifact suppression techniques and final image quality. Through an empirical testing process we determined that the MAD wavelet noise estimation technique is the overall preferred noise estimation technique for all noise artifact suppression techniques presented (BM3D, bilateral, Neighshrink, BLS-GSM and non-local means). We also found the BM3D noise artifact suppression technique, when combined with the MAD wavelet noise estimation technique, performed the best of the all noise artifact suppression techniques presented when an estimated noise level is used.

Acknowledgments

The authors would like to thank the Natural Sciences and Engineering Research Council (NSERC) of Canada, the GEOmatics for Informed DEcisions (GEOIDE) network, and the Ontario Centres of Excellence (OCE) for providing funds for this project.

References

[1] S. Chitchian, M. A. Fiddy, T. Weldon, and N. Fried, "Combined image-processing algorithms for improved optical coherence tomography of prostate nerves," *J. Biomed. Opt.*, vol. 15, p. 046014, 2010.

[2] W. Wang, "A perimeter-based noise filter algorithm for vehicle recognition," *Proc. International Symposium on Intelligent Ubiquitous Computing and Education*, pp. 42–45, 2009.

[3] W. Yang, B. Fang, Y. Tang, Z. Shang, and D. Li, "Sift features based object tracking with discrete wavelet transform," *Proc. International Conference on Wavelet Analysis and Pattern Recognition*, pp. 380–385, 2009.

[4] D. L. Donoho and I. M. Johnstone, "Ideal spatial adaptation by wavelet shrinkage," *Biometrika*, vol. 81, pp. 425–455, 1994.

[5] D. L. Donoho, "De-noising by soft-thresholding," *IEEE Transactions on Information Theory*, vol. 41, pp. 613–627, 1995.

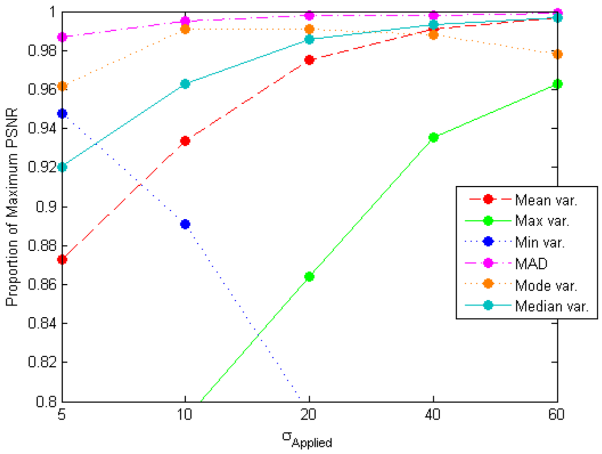

(a)

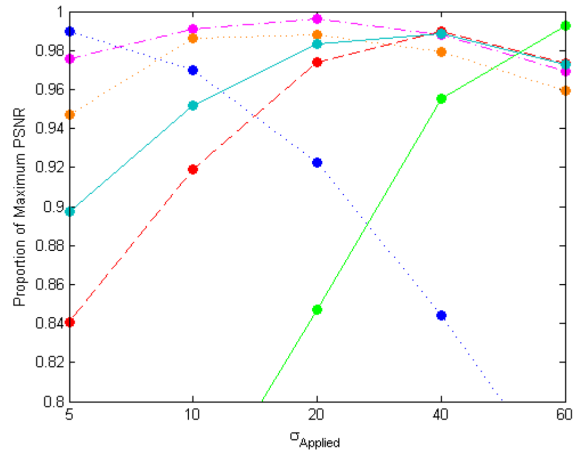

(b)

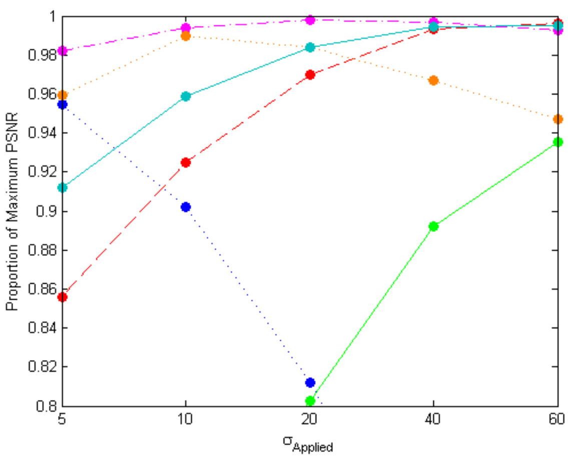

(c)

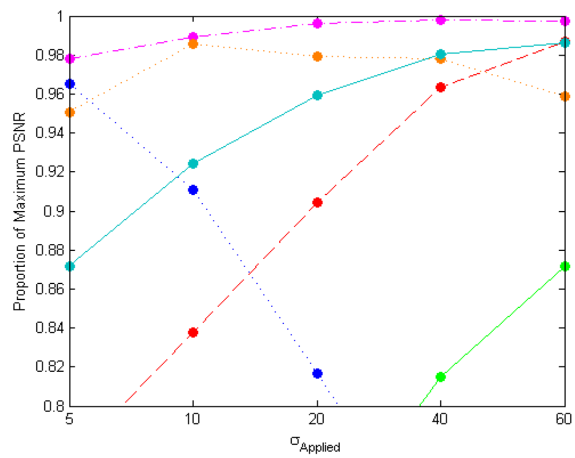

(d)

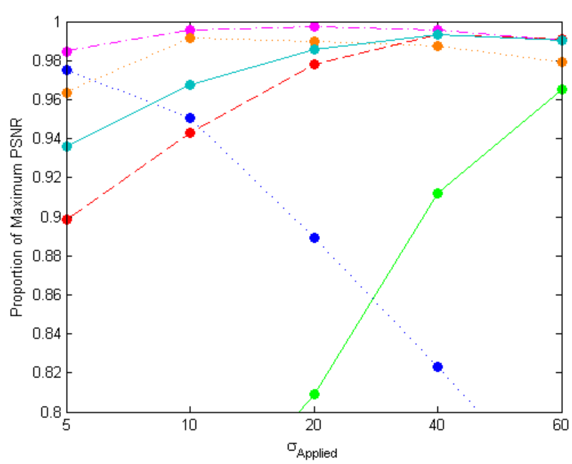

(e)

Figure 3. Performance of noise estimators when using the (a) BM3D (b) bilateral (c) Neighshrink (d) BLS-GSM or (e) non-local means noise artifact suppression techniques. Their performances are measured using the calculations shown in Equations (9) and (10). Note that some of the lower data points for the minimum variance and maximum variance techniques were cut off to provide greater resolution of the higher data points, which in this case are much more relevant since we are most concerned with highest data point in each applied noise level. Also, it should be noted that the reason for the general upwards trends as high noise levels are approached is because noise artifact suppression techniques are typically much more sensitive to using inaccurate input σ's in lower noise levels, whereas in high noise levels they tend to be much less sensitive. Thus the inaccuracies from the estimation techniques are less pronounced in the high noise levels.

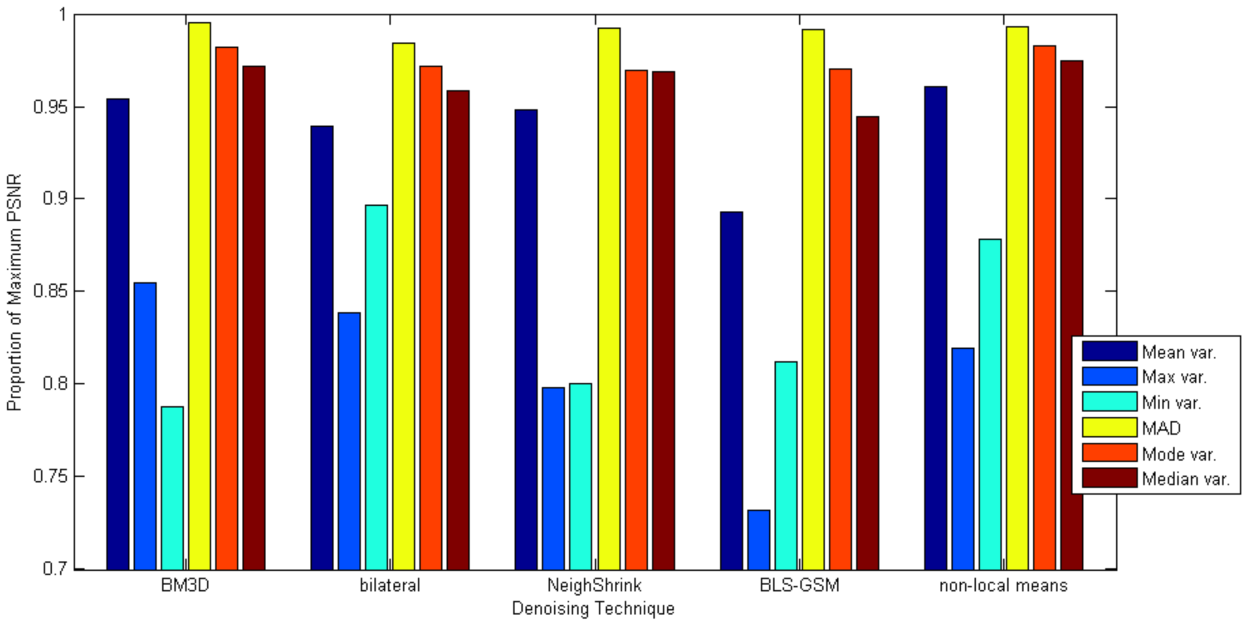

Figure 4. Performance of noise estimators when using each of the noise artifact suppression techniques with results averaged across all levels of applied noise.

[6] C. Tomasi and R. Manduchi, "Bilateral filtering for gray and color images," *Computer Vision, IEEE International Conference on*, vol. 0, p. 839, 1998.

[7] A. Buades, B. Coll, and J.-M. Morel, "A non-local algorithm for image denoising," *Computer Vision and Pattern Recognition, IEEE Computer Society Conference on*, vol. 2, pp. 60–65, 2005.

[8] J. Portilla, V. Strela, M. J. Wainwright, and E. P. Simoncelli, "Image denoising using gaussian scale mixtures in the wavelet domain," *IEEE Transactions on Image Processing*, vol. 12, pp. 1338–1351, 2002.

[9] Dabov, Foi, Katkovnik, and Egiazarian, "Image Denoising by Sparse 3-D Transform-Domain Collaborative Filtering," *Image Processing, IEEE Transactions on*, vol. 16, no. 8, pp. 2080–2095, 2007.

[10] S. G. Chang, B. Yu, and M. Vetterli, "Adaptive wavelet thresholding for image denoising and compression," *IEEE Transactions on Image Processing*, vol. 9, no. 9, pp. 1532–1546, Sep. 2000.

[11] C. Liu, W. Freeman, R. Szeliski, and S. Kang, "Noise estimation from a single image," *Computer Vision and Pattern Recognition, IEEE Computer Society Conference on*, pp. 901–908.

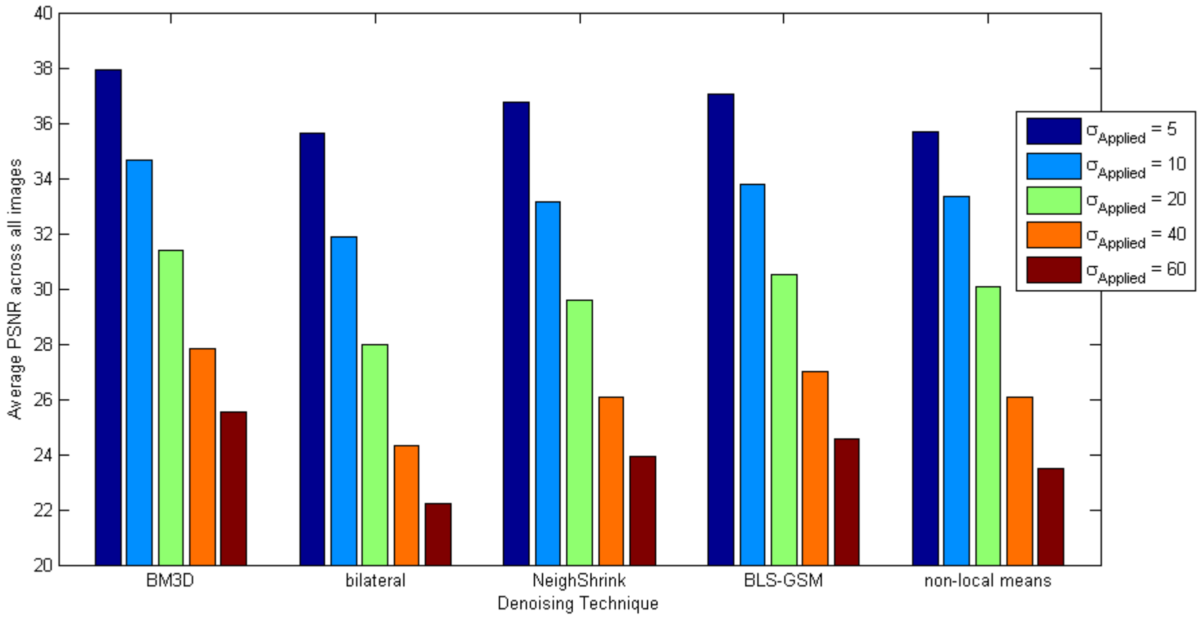

Figure 5. Performance of noise artifact suppression techniques when using an estimated noise level generated from the MAD estimator.